行政院國家科學委員會專題研究計畫　成果報告

三次元側向阻尼效應之研究與硬體描述語言模型之建立

計畫類別：個別型計畫
計畫編號：NSC91-2218-E-002-021-
執行期間：91 年 08 月 01 日至 92 年 07 月 31 日
執行單位：國立臺灣大學機械工程學系暨研究所

計畫主持人：楊燿州

計畫參與人員：顏柏青，鄭凱隆

報告類型：精簡報告

處理方式：本計畫可公開查詢

中　華　民　國 93 年 2 月 11 日

Macromodels of 3D Lateral Viscous Damping Effects for MEMS Devices

Po-Ching Yen and Yao-Joe Yang
Department of Mechanical Engineering
National Taiwan University
1 Roosevelt Rd. Sec 4., Taipei, Taiwan, ROC
pcyen@mems.me.ntu.edu.tw, TEL:+886 2 23646491 FAX:+886 2 23631755

ABSTRACT

In this work, a fast algorithm of generating accurate time-domain macromodels of viscous lateral damping for three-dimensional MEMS geometries is described. A three-dimensional finite-difference (FDM) Stokes flow solver for simulating lateral damping effects was developed. The system matrices generated by the solver was then reduced to low-order macromodels that can be easily inserted into a system-level modeling simulators, such as Saber, Simulink or SPICE for transient and frequency analysis. The macromodels have proved to be about three-order-of-magnitude as efficient as the FDM solver, while preserve the 3-D edge effects that usually require expensive 3-D BEM or FEM calculations. Experimental results of quality factors for comb-drive devices demonstrated that the error of the results estimated by the macromodels is within 15%.

Keywords: lateral viscous damping, model order reduction, macromodel, comb drive

INTRODUCTION

Many MEMS devices such as accelerometers, gyroscopes, switches, micro-mirrors, and resonant sensors need fully understanding of lateral gas damping effects for accurate dynamic modeling. It is well known that modeling 3-D lateral viscous damping effects requires considerable computational resources. For example, Figure 1 shows a typical comb-drive device whose mechanism is widely used as the core sensing or actuating structures for MEMS devices. The interdigital comb-shapes and the folded-beams are in fact very complicated geometrical structures. Furthermore, for 3D finite-element (FEM) or finite-difference (FDM) analysis of the air damping effects on the structure, the solid-model (meshes) is even more complicated, because the computational domain is the air-film surrounding the comb structures. Therefore, 3D FEM/FDM approaches not only require intensive solid-modeling work, but also require significant computational resources even for a steady incompressible-flow simulation. As a result, earlier works on lateral viscous damping were based on the 1-D analytical Stokes and Couette flow solutions [1,2,3]. The 1-D analytical approaches can easily provide the first-order estimation of lateral damping effect, and require almost zero computational resources so that they are intrinsically compatible with any system-level simulators. However, the 1-D approaches over-simplify the geometrical complexity of typical MEMS devices with lateral damping effects, and thus the error is very large in most cases.

Recently, Aluru and Wang [4,5] developed 3-D Stokes solvers using 3D boundary-element method (BEM). The 3D BEM approaches only need 2D panels (meshes) on the surfaces of any 3D structures, so the required solid-modeling works are relatively easy than the 3D finite-element approaches. Furthermore, with certain numerical acceleration techniques [6], the computation efficiency of the BEM approaches are much less than typical FEM/FDM approaches. However, since the governing equations solved by the BEM techniques are in frequency domain, the major limitation of the BEM approaches is that the simulated results are for a specific operating frequency, and thus are not completely compatible with transient system-level analysis.

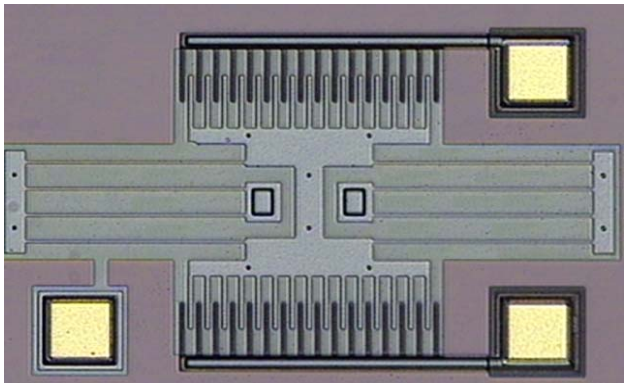

Figure 1. The CCD picture of a comb-drive (by MUMPs) simulated and measured in this work

In this work, we developed a model-order-reduction (MOR) methodology [7,8,9] for generating accurate time-domain macromodels from 3-D FDM/FEM formulations. The initial step of generating the macromodels is to

generate 3D solid models. This step is very similar to the typical procedure of performing FEM//FDM fluidic simulation. However, we used the commercially-available MEMS modeling packages, such as Coventorware, IntelliSuite and MEMS-Pro, to generate the 3D solid model of the air file from 2-D mask layout, by considering the air-film surrounding the structures as the fictitious sacrificial layer.

After creating the solid model of the air film surrounding a MEMS laterally-movable structure, the FEM/FDM techniques are used to discretize the solid model. Since the governing equation is in time domain, the discretization creates a system (set) of ordinary differential equations whose state variables are in fact the velocity distribution of the air film. Since the system is so large that huge computational resources for time-domain integration are required. Without direct integration of the system, an Arnoldi algorithm is applied to reduce the system of differential equations into a low-order system, the so-called macromodel. The macromodels can be readily inserted into system-level simulators, such as Saber® or Simulink®, for transient and frequency-response analysis.

In the following, the theory of the fluidic damping effects and the application of the model-order-reduction technique are first presented. Comparisons between the measured and simulated quality factors are demonstrated. Finally, the discussions between various approaches are presented.

THEORY

A. 3-D FDM Model

The governing equation of lateral viscous damping is the Stokes equation. The 3-D Stokes' equation is [10]:

$$\rho \frac{D\vec{V}}{Dt} = -\nabla p + \rho g + \mu \nabla^2 \vec{V} \tag{1}$$

where p is pressure, ρ is the density of the gas, μ is the viscosity coefficient, and $\vec{V} = [u \quad v \quad w]^T$ is the velocity vector. For our case, the imposed pressure gradient is assumed to be zero, so the first term on the right-hand side of Equation (1) is eliminated.

In order to further simplify the governing equation, we study the Reynolds number of the system:

$$\mathrm{Re} = \frac{\rho L U}{\mu} \tag{2}$$

where L is the characteristic dimension of the model. In our case, it is the gap between two laterally moving surfaces. U is the characteristic velocity of the fluid. Using typical parameters for thin-plate-type or comb-drive-type MEMS devices under in-plane motion (for example, L=2μm, U=1000μm/s), the Reynolds number is much less than 1. Under this condition, as discussed in [11], the second term on the right-hand side of Equation (1) can be eliminated. Finally, since the damping contributed by the surfaces, whose normal vectors are parallel to the direction of plate motion, is negligible under our assumptions ($u >> v \approx w$), the velocity components perpendicular to the direction of the in-plane motion are ignored. As a result, the continuity equation is not considered. Finally, the simplified equation that will be studied in this work is:

$$\frac{\partial u}{\partial t} = \upsilon \nabla^2 \mu = \upsilon \left(\frac{\partial^2 u}{\partial x^2} + \frac{\partial^2 u}{\partial y^2} + \frac{\partial^2 u}{\partial z^2} \right) \tag{3}$$

where $\upsilon = \mu / \rho$ is the kinetic viscosity. Based on this equation, a finite-difference solver is developed.

B. Arnoldi-based MOR Algorithm

Although the 3-D FDM Stokes solver is capable of solving the transient response of the damping effects of the MEMS devices, it requires significant effort on meshing the fluid surrounding the structure as well as huge computational resources on transient simulations. Fortunately, the governing equation, as shown in Equation (3), is a linear equation, and therefore the system matrices generated by FDM approximation process for Equation (3) can be reduced by an Arnoldi-based model-order-reduction (MOR) technique. The dynamic system equation formulated by the FDM approximation of Equation (3) can be written as:

$$\begin{aligned} \dot{\vec{u}} &= \mathbf{A} \cdot \vec{u} + \mathbf{B} \cdot v_{in} \\ \vec{y} &= \mathbf{C}^T \cdot \vec{u} + \mathbf{D} \cdot v_{in} \end{aligned} \tag{4}$$

where $\mathbf{A}$ is an n by n matrix and n is the total number of nodes, $\vec{u}$ is the vector which contains the unknown velocity distribution on each node, and the input function v_{in} is the imposed velocity on the moving boundary of the computational domain. In this case, we carefully formulate $\mathbf{C}$ and $\mathbf{D}$, so that the output $\vec{y}$ will be the frictional shear (calculated by Newtonian law of viscosity) on the plate. In Laplace domain, the transfer function of the system is:

$$\begin{aligned} T(s) &= \mathbf{C}^T (\mathbf{I}s - \mathbf{A})^{-1} \mathbf{B} + \mathbf{D} = \mathbf{C}^T (\mathbf{I} - s\mathbf{A}^{-1})^{-1} \vec{b} + \mathbf{D} \\ \vec{b} &= -\mathbf{A}^{-1} \mathbf{B} \end{aligned} \tag{5}$$

After expanding the transfer function in Taylor series about $s=0$, we obtain:

$$T(s) = \mathbf{C}^T (\mathbf{I} + s\mathbf{A}^{-1} + s^2 \mathbf{A}^{-2} + \ldots)\vec{b} + \mathbf{D} = \sum_{k=0}^{\infty} m_k s^k + \mathbf{D} \tag{6}$$

where m_k are the coefficients of the Taylor series, and are equal to $m_k = \mathbf{C}^T \left(\mathbf{A}^{-k} \right) \vec{b}$.

The Taylor expansion can be truncated to approximate the transfer function $T(s)$. Since $\mathbf{A}^{-k}\vec{b}$ quickly line up with a single eigenvector, this moment matching procedure is usually numerically unstable. Therefore, we apply the Arnoldi-based algorithm to stably compute orthogonal bases v_i that spans the Krylov subspace:

$$K_q\left(\mathbf{A}^{-1},\vec{b}\right)=span\left\{\vec{b},\mathbf{A}^{-1}\vec{b},\mathbf{A}^{-2}\vec{b},\cdots,\mathbf{A}^{-(q-1)}\vec{b}\right\} \quad (7)$$

Given the matrix $\mathbf{V_q}$ whose columns are $\{v_i\}$, the Arnoldi algorithm reduces the system matrix $\mathbf{A}$ to a small upper Hessenberg matrix $\mathbf{H_q}$ whose entries are the Gramm-Schmidt orthogonalization coefficients:

$$\mathbf{V_q}^{\mathbf{T}}\mathbf{A}\mathbf{V_q}=\mathbf{H_q} \quad (8)$$

Finally, the reduced transfer function can be written as:

$$T_q(s)=\mathbf{C}^T\mathbf{V_q}\left(\mathbf{I_q}-s\mathbf{H_q}\right)^{-1}\mathbf{V_q}^T\vec{b}+\mathbf{D} \quad (9)$$

Note that the reduced system transfer function, as shown in Equation (9), has the same input (v_{in}) and output ($\vec{y}$) as those in Equation (4). Since the typical sizes of the system matrices are very small, the computational efficiency for simulating transient responses and frequency responses of the reduced models are significantly increased.

RESULTS

A. Comparison of Simulated FDM and Macromodel Results

Figure 1 shows the picture of the simulated and measured comb drive structure fabricated by the MUMPs® process. Because of the symmetric geometry of the device, the solid model of the air films surrounding one quarter of the structure is created. The total number of the nodes after discretizing the air films is more than 500,000. The gas properties used in this work are μ=18.5 x 10^{-6} Ns/m^2, ρ=1.1766 kg/m^3 and υ=15.73x10^{-6} m^2/s. Figure 2 shows that when the device moves with constant velocity u = 1000 μm/s, the transient response of the total shear forces surrounding the plate calculated by the FDM solver decreases from 2.7x10^{-4} μN to a steady state value of 8.5x10^{-5} μN at about 10^{-7} sec. Note that in Figure 2, the result by the 1-D Couette flow solution underestimates the damping forces due to neglecting the edge/end effects. Figure 3 shows the relative errors of the simulation results between different orders of the macromodels and the FDM solver. The figure indicates that the steady state error between each macromodel and the FDM solver converges to about 0.1%, while the transient response error (before 2.0 x 10^{-7} sec) are heavily depends on the order of the macromodel. The discrepancy between the 2nd macromodel result and the FDM result is about 7 %, but the 10th order macromodel result match with the FDM result very well (within 2%). The error decreases as the order of the macromodel increases. The speed-up factors of the macromodels are shown in Table 1. The average improvement of computational performance is at least 1,000 times.

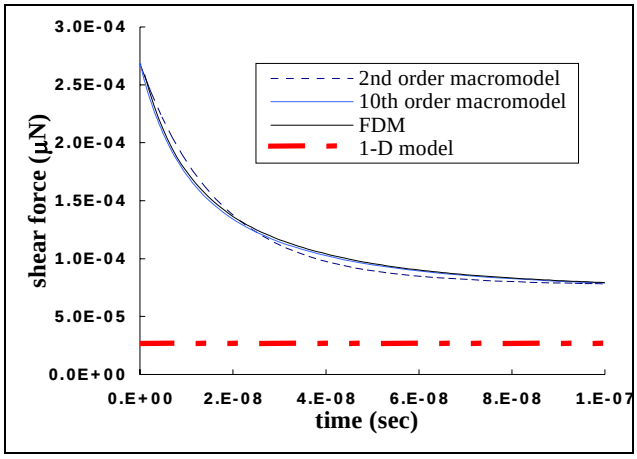

Figure 2. The results of transient simulations of the FDM solver and the macromodels. The simulated velocity of the moving comb structure is 1000 μ/s.

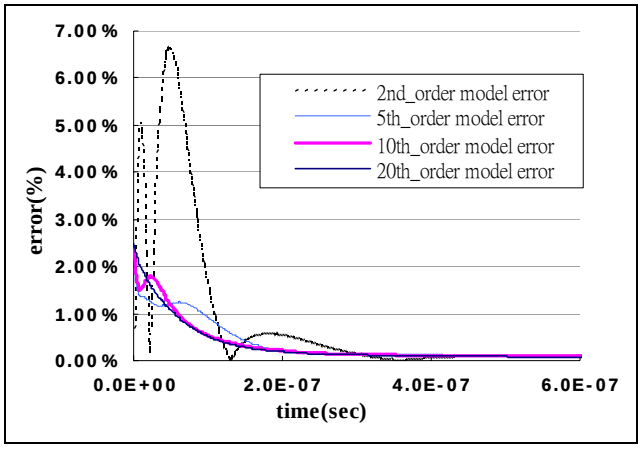

Figure 3. The error between the macromodels and the FDM solver results.

Results by the FDM Solver (full model)

Simulation time (=F)	195 sec

Results by the Macromodel (reduced models)

Types	**2nd order**	**5th order**	**10th order**	**20th order**
Model generating time	29.69 sec	46.47 sec	76.62 sec	115.33 sec
Simulation time (=R)	0.013 sec	0.025 sec	0.051 sec	0.103 sec
Speed-up factor (=F/R)	15000	7800	3823	1893

Table 1. Comparison of simulation times by the FDM solver and the macromodels with different orders, as well as the speed up factors.

B. System-level Simulation and Comparison with Measured Results

The macromodels generated by the Arnoldi-based MOR algorithm can be readily inserted into system-level simulators, such as Saber® or Simulink®, for transient and frequency-response analysis. Figure 4 shows a Simulink® system block diagram, which shows that a lateral damping macromodel is inserted into a 2nd-order dynamic system. This diagram is typical for simulating a comb drive with one degree-of-freedom motion. Table 2 shows the effective mass, effective spring constant and the dimensions for the six different devices studied in this work. Figure 5 shows the simulated and measured comb-drives quality factors vs. different folded-beam lengths (see Table 2). The figure presents that the 1-D Stokes/Couette models over-predicts the quality factors by 30~40%, while the discrepancy between the measured results and the macromodels is within 15%.

CONCLUSION

This paper presented a macromodel generation methodology for lateral damping effects based on the Arnoldi-based model-reduction technique. The theory of the Arnoldi-based model-order-reduction is described, and the comparison of errors and speed up factors for macromodels with different orders were also provided. The macromodels generated by the technique were successfully inserted into the Simulink for system level analysis, and the results were also compared with the experimental data. The macromodels are at least 1000 times faster than FDM/FEM solvers. The discrepancy of the simulated and measured quality factors are within 15%.

Beam width (μm)	2	2	2	2	2	2
Beam length (μm)	168	180	192	204	216	228
Structure thickness (μm)	2	2	2	2	2	2
Finger width (μm)	3	3	3	3	3	3
Finger length (μm)	40	40	40	40	40	40
Finger gap (μm)	3	3	3	3	3	3
Finger overlap (μm)	20	20	20	20	20	20
Effective mass (μg)	0.0429	0.0433	0.0436	0.0439	0.0443	0.0446
Effective spring constant (μN / μm)	0.9448	0.7682	0.6330	0.5277	0.4446	0.3780

Table 2. The dimensions of the comb drive devices studied in this work.

ACKNOWLEDGEMENT

This research was supported by the National Science Council (Grant No. 91-2218-E-002-021), Taiwan, R.O.C.

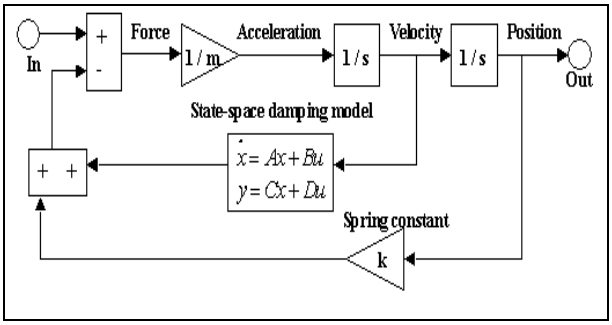

Figure 4. A Simulink® system level schematic with a lateral damping macromodel.

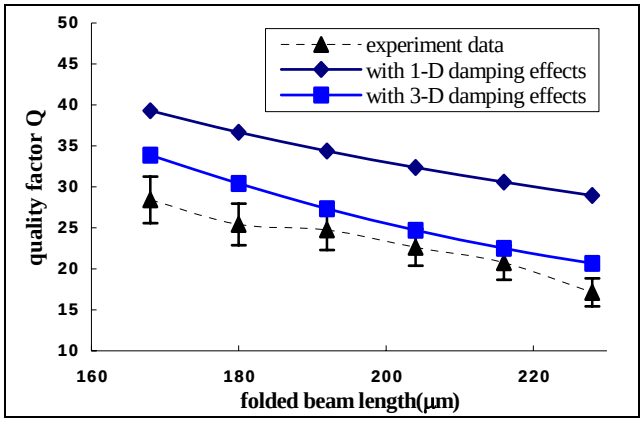

Figure 5. Comb-drive quality factors vs. different folded-beam lengths.

REFERENCES

1. Y.-H. Cho, et. al., "Viscous Damping Model for Laterally Oscillating Microstructures," J. MEMS, vol. 3, no. 2, June 1994, pp. 81-87.
2. X. Zhang, et. al., "Viscous Air Damping in laterally driven microresonator," Sensors and Materials, vol. 7, no. 6, pp. 415-430, 1995.
3. T. Veijola, "Compact Damping Models for Lateral Structures Including Gas Rarefaction Effects,"
4. N. R. Aluru, et. al., "A fast integral equation technique for analysis of microflow sensors based on drag force calculations," Proc. Of MSM, 283-286, 1998.
5. X. Wang, M. Judy, and J. White, "Validating Fast Simulation of Air Damping in Micromachined Devices," Proceeding of MEMS 2002, Jan. 2002, Las Vegas, USA.
6. W. Ye, et. al., "Viscous Drag on A Lateral Micro-Resonator: Fast 3-D Fluid Simulation and Measured Data", Tech. Digest, Solid-State Sensor and Actuator Workshop, Hilton Head Island, SC, June 2000, pp 124-127.
7. Y.-J. Yang, et. al. "Modeling Gas Damping and Spring Phenomena In MEMS With Frequency Dependent Macro-Models" IEEE MEMS 2001.
8. A. Odabasioglu, et. al., "PRIMA," IEEE Transaction on Computer-Aided Design of Integrated Circuits and Systems, Vol. 17, No. 8, August 1998.
9. P.-C. Yen and Y.-J. Yang, "Time-Domain Reduced-Order Models of Lateral Viscous Damping Effects for 3-D Geometries", MSM 2002, San Juan, Puerto Rico, USA, Apr, 2002, pp 190-193.
10. J. A. Fay, Introduction to Fluid Mechanics, MIT Press, Cambridge, 1994.
11. M. C. Potterm, D. C. Wiggert, Mechanics of Fluids, 2nd Edition, Kluwer Academic Publishers.